AIP | Journal of Applied Physics

Optical properties of In1−x Ga x P1−y As y , InP, GaAs, and GaP determined by ellipsometry

H. Burkhard, H. W. Dinges, and E. Kuphal

Citation: Journal of Applied Physics **53**, 655 (1982); doi: 10.1063/1.329973
View online: http://dx.doi.org/10.1063/1.329973
View Table of Contents: http://scitation.aip.org/content/aip/journal/jap/53/1?ver=pdfcov
Published by the AIP Publishing

Articles you may be interested in

Electrical properties of modulation-doped In x Al 1−x As/In y Ga 1−y As structures on GaAs and InP substrates with 0.2x, y0.8
J. Vac. Sci. Technol. B **18**, 1633 (2000); 10.1116/1.591442

Band gap modification in Ne+-ion implanted In 1−x Ga x As/InP and InAs y P 1−y /InP quantum well structures
J. Appl. Phys. **81**, 765 (1997); 10.1063/1.364440

Optical dispersion relations for GaP, GaAs, GaSb, InP, InAs, InSb, Al x Ga1−x As, and In1−x Ga x As y P1−y
J. Appl. Phys. **66**, 6030 (1989); 10.1063/1.343580

Influence of interface quality on structural and optical properties of Ga x In1−x As/Al y In1−y As superlattices lattice matched to (001) InP
J. Appl. Phys. **66**, 3217 (1989); 10.1063/1.344138

Optical properties of molecular beam epitaxially grown GaAs1−x Sb x (0x
J. Appl. Phys. **63**, 5859 (1988); 10.1063/1.340274

[This article is copyrighted as indicated in the article. Reuse of AIP content is subject to the terms at: http://scitation.aip.org/termsconditions. Downloaded to] IP: 35.8.11.3 On: Wed, 27 Jan 2016 02:10:42

Optical properties of $In_{1-x}Ga_xP_{1-y}As_y$, InP, GaAs, and GaP determined by ellipsometry

H. Burkhard, H. W. Dinges, and E. Kuphal
Forschungsinstitut der Deutschen Bundespost beim FTZ, D 6100 Darmstadt, Federal Republic of Germany

(Received 30 June 1981; accepted for publication 15 September 1981)

Refractive indices and absorption coefficients of $In_{1-x}Ga_xP_{1-y}As_y$ for $y = 0$ to 1 lattice matched to InP and of GaAs and GaP have been measured by ellipsometry in the wavelength range between 365 and 1100 nm. The high-purity layers ($7\times10^{14} < n < 2\times10^{16}$ cm^{-3}) used here were grown by liquid phase epitaxy. The quaternary refractive indices were also calculated from the measured indices of the constituent binary compounds by averaging the quantity $(\epsilon - 1)/(\epsilon + 2)$. The ϵ values were all taken at the same energy separation from the respective band gaps. The results of this new averaging procedure are compared with the measured indices and with the refractive index steps to InP deduced from lasers. In addition, the absorption coefficient of InP near the band gap was measured as a function of the doping level. Finally, the temporal growth of the natural oxide layer thickness d_{ox} on various InP and GaAs samples was determined by ellipsometry. For InP, the increase of d_{ox} is 0.39 nm per decade of time.

PACS numbers: 78.65.Jd, 68.55. + b, 07.60. − j, 81.60. − j

I. INTRODUCTION

InP and its related alloys $In_{1-x}Ga_xP_{1-y}As_y$ and $In_{0.53}Ga_{0.47}As$ lattice matched to InP have gained considerable interest for various microwave and optoelectronic devices. Precise values of the refractive index n and the absorption constant α of these alloys are needed for proper device tailoring. In photodetectors the efficiency as a function of wavelength λ strongly depends on $\alpha(\lambda)$. In double heterostructure (DH) lasers the optical far field and the threshold current are functions of the refractive index step Δn of the quaternary active layer relative to the InP cladding layers. Limited and contradictory information on Δn is available from studies of the far-field pattern of lasers.[1–4] We have investigated, therefore, the optical constants of $In_{1-x}Ga_xP_{1-y}As_y$ single layers in the wavelength range from 365 to 1100 nm for y between 0 and 1. The parameter x is determined by the condition of lattice matching to InP. To our knowledge, no direct measurements of n and α have been performed in this range up to now. There is only one paper on n covering the range $\lambda > 1150$ nm.[5]

For the binary constituents of $In_{1-x}Ga_xP_{1-y}As_y$ refractive index measurements are reported in the literature: InP[6,7]; GaAs[8–10]; GaP[11]; InAs.[8] For InP, GaP, and GaAs we have repeated these measurements, as the published data are partly contradictory. The technique used here was ellipsometry, supplemented by photoluminescence measurements on InP in the vicinity of the band gap energy. The material investigated was grown by liquid phase epitaxy in our laboratory.

The most reasonable way to calculate the quaternary refractive indices from the measured binary compound data will be shown to be an averaging process of the quantity $(\epsilon - 1)/(\epsilon + 2)$ according to Vegard's rule, where ϵ is the dielectric constant. In order to get an ϵ value of the quaternary compound at an energy separation ΔE from the band gap, the ϵ values of the binaries have to be taken at the same ΔE from their respective band gaps. This procedure was justified by the fact that the refractive indices of all binary as well as quaternary materials exhibit a very similar shape when plotted versus the energy separation from their respective band gaps.

II. EXPERIMENTAL PROCEDURE

A. Liquid-phase-epitaxial growth

The investigated layers of InP, InGaAs, InGaPAs, and GaAs were prepared by liquid phase epitaxy (LPE) in multiple-bin sliding boat systems. The first three materials were grown on (100)-oriented InP substrates, whereas GaAs was grown on (100)-oriented GaAs substrates. Thicknesses were between 2 and 7 μm. All layers except those used for Fig. 6 were nominally undoped. The background doping level was between 7×10^{14} and 2×10^{16} cm^{-3}, see Table I. These low levels are due to a long-term prebake of the source materials[16]. Prior to growth the thermally degraded InP substrate was melted back by an undersaturated In-InP solution. For the growth of GaAs, InP, and InGaAs slightly oversaturated melt compositions were chosen, whereas for InGaPAs the two-phase solution technique with excess InP was applied. Starting temperatures were 730 °C for the growth of GaAs and 630 °C for the compounds on InP substrates, the cooling rate being 10 °C/h throughout.

The lattice mismatch, which was determined by x-ray diffraction, could be reduced by optimization of the liquid composition to $<4\times10^{-4}$ for each mixed crystal composition. The mixing parameters x and y indicated in Table I were independently determined by electron microprobe analysis with an accuracy of ± 0.01. The observed relation between x and y is in accordance with the function given by Hsieh.[17]

B. Reflection ellipsometry

The refractive index n and the absorption coefficient k were measured by reflection ellipsometry. The wavelengths used were selected by interference filters of 2 nm halfwidth.

 0021-8979/82/010655-08$02.40 © 1982 American Institute of Physics

[This article is copyrighted as indicated in the article. Reuse of AIP content is subject to the terms at: http://scitation.aip.org/termsconditions. Downloaded to] IP: 35.8.11.3 On: Wed, 27 Jan 2016 02:10:42

TABLE I. Composition, doping level, and band parameters of the layers used in this study. All materials except GaP were grown by LPE. The GaP sample is p-type VPE material. The band parameters are discussed in Sec. III. A.

Compound		$N_D - N_A$ (cm^{-3})	E_0 (eV)	$E_1 + \Delta_1$ (eV) This work	Published data
GaAs		7×10^{14}	1.425	3.12	3.12 (Ref. 12)
GaP		7×10^{16}	2.26 (ind.) 2.77 (dir.)		
$In_{1-x}Ga_xP_{1-y}As_y$					
y	x				
0	0	1.4×10^{15}	1.35	3.25	3.27 (Refs. 13 and 14) 3.26 (Ref. 15)
0.54	0.24	1×10^{16}	0.99	2.97	3.00 (Ref. 13 and 15)
0.61	0.27	2×10^{16}	0.95	2.95	2.97 (Ref. 13 and 15)
0.70	0.31	1.8×10^{15}	0.90	2.93	2.93 (Ref. 13 and 15)
1.00	0.47	2×10^{15}	0.75	2.82	2.82 (Ref. 13) 2.80 (Ref. 15)

The upper limit of the wavelength range was 1040 nm, caused by the used S1 photomultiplier. The angle of incidence φ_0 was 70°, but other values were also used for consistency checks. Care was taken to measure in the wavelength range, where the penetration depth of the light is smaller than the epitaxial layer thickness, so that the substrate does not affect the measurements.

Interference effects in the natural oxide layer on our samples were taken into account in the analysis. This was proved to be necessary, since an oxide layer of thickness $d_{ox} = 5$ nm and refractive index $n_{ox} = 1.9$ changes the apparent refractive index by $\delta n = -0.03$ (for $n = 3.6$, $\lambda = 546$ nm). This error even increases with n. We assumed the oxide layer to be absorption free and homogeneous. A similar sensitivity of n on the oxide thickness also exists for the usual reflection technique with unpolarized light.

The dependence of the ellipsometric angles Ψ and Δ on the preset parameters (λ, φ_0), on the epitaxial layer parameters (n, k) and on the oxide layer parameters (n_{ox}, d_{ox}) is governed by a set of transcendental equations given, e.g., in Ref. 18. This system of equations, which was solved numerically, is initially not fully determined, since there are only two measured quantities (Ψ, Δ) against four unknown parameters (n, k, n_{ox}, d_{ox}). Therefore, assumptions were needed about two of the parameters. For GaAs, $n_{ox} = 1.9$[19] and $k = 0.304$[20] are known at the "standard" ellipsometric wavelength $\lambda = 546.1$ nm. Hence, n and d_{ox} could be determined. For different wavelengths, d_{ox} is, of course, the same, and n_{ox} was taken to be unchanged. Therefore, n and k could be deduced as a function of λ. For InP the following procedure was applied: We assumed that the natural oxide in InP is essentially In_2O_3, whose refractive index varies between 2.1 and 1.9 over the wavelength range of interest.[21] The absorption coefficient of InP at $\lambda = 546$ nm is $k = 0.38$.[6] For InGaAs and InGaPAs no such values are known. However, since we found that GaAs and InP layers exhibit an oxide thickness $d_{ox} \sim 1.0$ nm 10 min after the end of their growth, we assumed the same oxide thickness for freshly grown ternary and quaternary layers, and used $n_{ox} = 1.9$ throughout. In this way, n and k were measured 10 min after growth at the standard wavelength. From measurements performed later on, the increased oxide thickness could easily be calculated using the initial n and k values. Measurements at different wavelengths could then be evaluated taking the actual d_{ox}.

The evaluation described above gives a very good approximation for n, since for a given pair Ψ, Δ the correlation between apparent n and n_{ox} (for $d_{ox} < 6$ nm) is only $\delta n/\delta n_{ox} = 0.02$.[22] Our overall precision in the index values is $\Delta n = \pm 0.01$. The correlation between k and d_{ox} is, however, strong (the apparent k increases with decreasing d_{ox}). While the relative dependence $f\,k\,(\lambda)$ is measured precisely, the absolute error in both k and d_{ox} is estimated to be 20%.

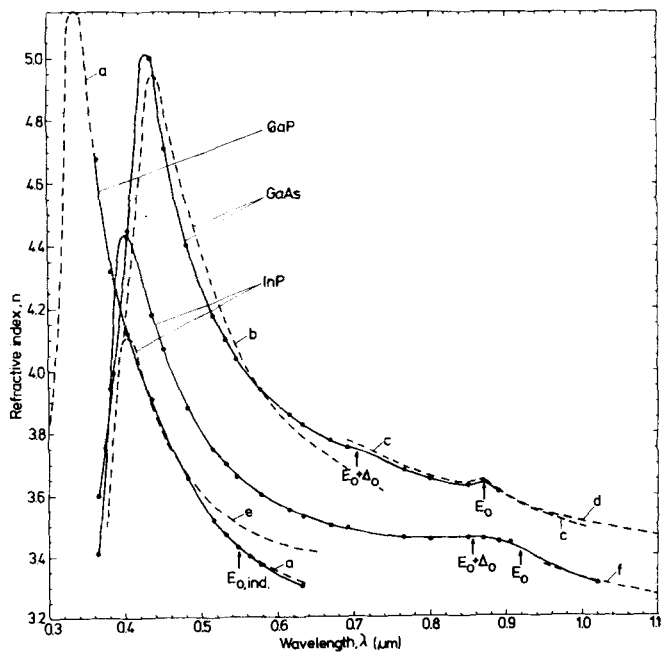

FIG. 1. Refractive indices vs wavelength of LPE GaAs, InP, and GaP (solid lines) compared to literature data (dashed lines). Curve (a) Ref. 11 for GaP; curves (b) Ref. 8, (c) Ref. 10, and (d) Ref. 9 for GaAs; curves (e) Ref. 6 and (f) Ref. 7 for InP. The band gap energies E_0 and the spin-orbit splitting Δ_0 are also indicated.

[This article is copyrighted as indicated in the article. Reuse of AIP content is subject to the terms at: http://scitation.aip.org/termsconditions. Downloaded to] IP: 35.8.11.3 On: Wed, 27 Jan 2016 02:10:42

III. RESULTS AND DISCUSSION

A. Refractive index data

The measured refractive indices of the binary compounds GaAs, InP, and GaP are compared with literature data in Fig. 1. The solid lines interconnect our measured values (dots), the dashed lines represent literature values. The refractive index of GaAs is governed by a strong resonance, which we attribute to the $E_1 + \Delta_1$ transition, and two weak maxima at E_0 and $E_0 + \Delta_0$. E_0 is the gap energy $\Gamma_{1c} - \Gamma_{15v}$, E_1 is attributed to the $L_{1c} - L_{3v}$ transition,[23] and Δ_0 and Δ_1 are the corresponding spin-orbit splittings. The measured n of high-purity GaAs ($N_D - N_A = 7\times10^{14}$ cm^{-3}) agrees exactly with that of Aspnes *et al.*[35] in the whole wavelength range and with that of Sell *et al.*[10] in the overlapping region (690–870 nm), and agrees with Ref. 24 below 600 nm. However, in the region between 600 and 730 nm the n values of Ref. 24 deviate to lower values compared to ours and to those of Refs. 10 and 35.

For InP the n values are shown with those of Cardona[6] and of Pettit and Turner.[7] In the short wavelength range we found much larger values of n than Cardona, especially our $E_1 + \Delta_1$ maximum is $n = 4.45$ compared to 4.10.[6] This discrepancy could possibly be due to the Kramers-Kronig analysis of the reflectance data in Ref. 6. Good agreement, however, is found in the overlapping region (> 950 nm) with Ref. 7. Their measurements on a bulk InP prism are considered to be very precise. As the spin-orbit splitting Δ_0 in InP is very small,[13] it could not be resolved here in contrast to GaAs.

For GaP exact agreement with the results of Morgan[11] in the range from $\lambda = 365$–632 nm is obtained. The refractive index values of the system InGaPAs are collected in Fig. 2. With increasing y the maxima due to the $E_1 + \Delta_1$ transition shift to longer wavelengths, and the refractive indices for $\lambda > 0.5\ \mu$m are a monotonically increasing function of y.

Table I summarizes the compositions and carrier concentrations of all samples together with the E_0 and $E_1 + \Delta_1$ transitions. The transition energies given in the last entry are derived from the peak positions of $\epsilon_2 = 2nk$, where n was taken from Figs. 1 and 2, and k from Fig. 5. Note that the maxima of ϵ_2 must be at higher energies than those of n. The comparison with literature data shows that our measured transition energies correspond very well to the $E_1 + \Delta_1$ transitions. The spin-orbit splitting Δ_1 could not be resolved.

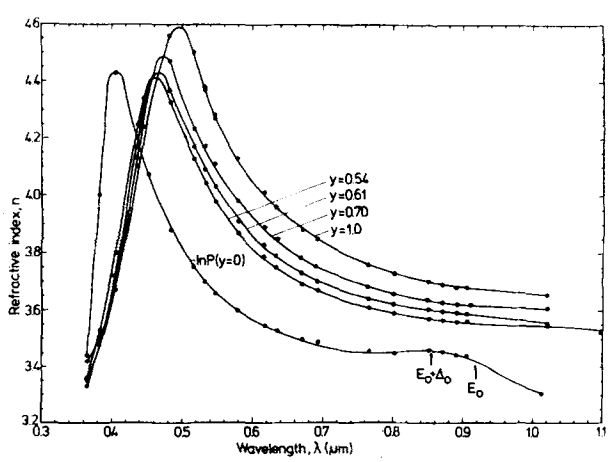

FIG. 2. Refractive indices vs wavelength of the system $In_{1-x}Ga_xP_{1-y}As_y$. The experimental points are averages over several samples.

B. Calculation of the quaternary refractive indices

For the design of DH lasers it is very useful to have an analytical expression for the refractive index n_Q of $In_{1-x}Ga_xP_{1-y}As_y$ as a function of y and of photon energy E. Various attempts have been made in the literature to calculate the n_Q from the binary data using Vegard's rule for a physical quantity X

$$X(In_{1-x}Ga_xP_{1-y}As_y) = (1-x)(1-y)X(InP) + (1-x)yX(InAs) + x(1-y)X(GaP) + xyX(GaAs). \quad (1)$$

Some authors[25,26] have averaged with this formula taking for X the band gap refractive indices of the four constituent binaries. Since the refractive index is in principle not an additive quantity, we think that this procedure is not justified. To average the dielectric constants, as was done in Ref. 27, has also no physical basis, as only susceptibilities—which means $(\epsilon - 1)$—are additive. To take the susceptibility instead of ϵ for the quantity X would already be a better approach, but is in principle only justified for low densities of dipoles, where the local electric field is identical to the macroscopic field. In another attempt[27] the single oscillator parameters E_0, E_d, and E_g of the binaries are interpolated according to Eq. (1), and in a subsequent step the modified single oscillator model for the refractive index[28] is applied. Since even the description of the binary refractive indices by this model in the near band gap region is insufficient, it is not to be expected that the quaternary indices are realistic.

We believe that the best way to yield reliable quaternary refractive indices is to average the quantity $(\epsilon - 1)/(\epsilon + 2)$. This is based on Clausius-Mosotti's relation being the result of a summation of atomic polarizabilities of densely packed atoms. The relation of Clausius and Mosotti was extended to mixtures of binary compounds by Harrison and Hauser.[29] This model takes into account the change of the polarizabilities of the binary molecules due to the changed equilibrium interatomic spacing, with the consequence that the number of dipoles per unit volume occurring in Clausius-Mosotti's relation is canceled out. Thus, Eq. (1) may be applied to the quantity $X = (\epsilon - 1)/(\epsilon + 2)$, from which n_Q can directly be calculated taking $n^2 \approx \epsilon$. This interpolation scheme has already been used by Sasaki *et al.*[30] But these authors have used only relative permittivities without specifing the wavelength and without considering any spectral dependence.

We have calculated, for the first time, the energy dependence of n_Q. For that purpose we have taken our measured refractive indices of the binaries at an energy separation $\Delta E = E - E_0$, where E_0 is the respective band gap. The n_Q (ΔE) resulting from Eq. (1) is then yielded for the same energy separation ΔE from the quaternary band gap under consideration. In Fig. 3 our measured refractive indices of the binary and quaternary compounds are drawn as functions of ΔE. Only the values for InAs have been taken from litera-

[This article is copyrighted as indicated in the article. Reuse of AIP content is subject to the terms at: http://scitation.aip.org/termsconditions. Downloaded to] IP: 35.8.11.3 On: Wed, 27 Jan 2016 02:10:42

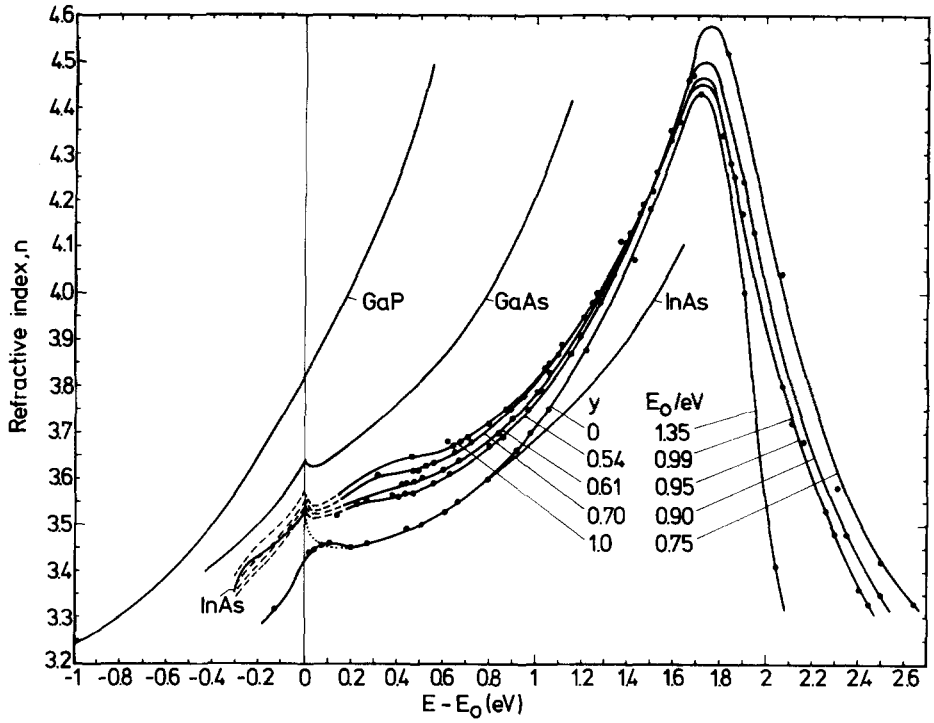

FIG. 3. Refractive indices vs energy separation $E - E_0$ of GaAs, GaP, and of $In_{1-x}Ga_xP_{1-y}As_y$ taken from Figs. 1 and 2 and of InAs from Ref. 27. The E_0 values used for $In_{1-x}Ga_xP_{1-y}As_y$ are indicated in the figure, the E_0 values used for GaAs, GaP, and InAs are 1.425 eV, 2.77 eV (direct gap) and 0.36 eV, respectively. The dotted part of InAs is estimated. For the quaternaries the dashed part is calculated as described in the text.

ture.[24] As GaP is a semiconductor with an indirect gap, but all quaternary compositions lattice matched to InP are direct, we also used for GaP the direct gap $E_0 = 2.77$ eV in Fig. 3. It becomes evident that the shapes of the curves for all materials are much more similar as compared to the presentation in Figs. 1 and 2. Not only the range near E_0 has become very similar, but also the peak positions due to the $E_1 + \Delta_1$ transitions nearly coincide at $\Delta E = 1.73$ eV for all InGaPAs compositions. We take this behavior as a justification for averaging properties of the binaries at a fixed energy separation ΔE from the respective band gaps.

The values of $n_Q(\Delta E, y)$ of undoped materials calculated following the above described procedure for -0.3 eV $< \Delta E < 0.2$ eV are drawn as dashed lines in Fig. 3. For $\Delta E > 0$ they join well the measured curves. For larger energies the interpolation scheme has not been applied, since the Clausius-Mosotti relation is not necessarily valid in the case of strong absorption. For -0.2 eV $\leqslant \Delta E \leqslant 0$, n_Q may be represented as functions of ΔE (in eV) and y from 0 to 1 as

$$n_Q(\Delta E, y) = 3.425 + 0.940\Delta E + 0.952(\Delta E)^2 + (0.255 - 0.257\,\Delta E)y - (0.103 - 0.0952\Delta E)y^2. \quad (2)$$

Equation (2) approximates the data of Fig. 3 to better than 0.01. The corresponding index describing the group velocity $\bar{n}_Q(\Delta E, y) = n_Q + E(dn_Q/dE)$ obtained from Eq. (2) is

$$\bar{n}_Q(\Delta E, y) = 3.425 + 1.88\Delta E + 2.86(\Delta E)^2 + (0.255 - 0.514\Delta E)y - (0.103 - 0.184\Delta E)y^2 + 0.94\,E_0 + 1.9E_0\Delta E - 0.257E_0y + 0.092E_0y^2. \quad (3)$$

Expressions (2) and (3) are of practical importance for quaternary lasers which emit at an energy slightly below the band gap. Note, however, that the effect of doping and carrier injection on n is not included here.

In Table II we have collected n_Q at the lasing wavelength and the index step to InP for some y values published by different authors. The agreement of our data with those of Refs. 2, 3, 5, and 25 is good. The far-field experiments on lasers of Henshall *et al.*[1] and Oomura *et al.*[4] yield index steps which in our opinion are too low. The fit to the far-field pattern in Oomura's work is not satisfactory and may therefore yield an unreliable result. The data of Buus and Adams[27] are systematically too low. For a comparison we have calculated the binary refractive indices from the modified single oscillator model[28] using their parameters.[27] These values are plotted in Fig. 4 as thin lines together with the experimental curves (thick lines) taken from Fig. 3. The agreement with the measured curves, especially for GaP and InP, is rather poor. Thus, one cannot expect satisfactory results for the quaternary system.

C. Absorption coefficients

The absorption coefficients obtained from ellipsometry of the same materials as in Figs. 1 and 2 are presented in Fig. 5. The data are again plotted against $\Delta E = E - E_0$, thus revealing the similarity of the different materials. For GaAs

[This article is copyrighted as indicated in the article. Reuse of AIP content is subject to the terms at: http://scitation.aip.org/termsconditions. Downloaded to] IP: 35.8.11.3 On: Wed, 27 Jan 2016 02:10:42

TABLE II. Quaternary refractive indices and index steps to InP for different laser wavelengths. Our own values are calculated from Eq. (2) with $\Delta E = -0.03$ eV.

y	$\lambda_{Laser}/\mu m$	n_Q	$n_Q - n_{InP}$	Reference
0.40	1.15	3.36	0.11[a]	1
		3.48	0.23	25
		3.40	0.15	27
		3.48	0.23	This work
0.47	1.20	3.496	0.27	25
		3.41	0.18	27
		3.37	0.14[a]	4
		3.49	0.26	This work
0.54	1.25	3.51	0.29	25
		3.52	0.30[a]	3
		3.42	0.19	27
		3.51	0.29	This work
0.61	1.31	3.53	0.31	25
		3.52	0.30[a]	2
		3.43	0.21	27
		3.52	0.31	5
		3.52	0.30	This work
1.00	1.65	3.56	0.40	25
		3.49	0.32	27
		3.56	0.40	5
		3.55	0.39	This work

[a]Results of far-field patterns of lasers.

($n = 7\times10^{14}$ cm^{-3}) our data agree well with Ref. 24 for $\Delta E > 0.5$ eV and are also in good agreement with the high-purity GaAs curve measured by Casey *et al.*[31] for $\Delta E < 0.2$ eV, while the data of Ref. 24 in this spectral range tend to be too low. For InP ($n = 1.4\times10^{15}$ cm^{-3}) our results coincide with those of Cardona[6] for $\Delta E > 0.3$ eV, but a noticeable discrepancy occurs between 0.1 and 0.3 eV.

The GaP curve has been shifted by the amount of the indirect energy gap. The shape is different as compared with the other curves on account of the different band structure. The absorption coefficients are in good agreement with another ellipsometric study on GaP.[11] For the quaternary system the absorption constant is found to increase monotonically with decreasing y for a fixed ΔE. Considering the vicinity of E_0 this can easily be understood because of the increase of the effective mass and thus the density of states with decreasing y.

In Fig. 6 the E_0 absorption edge of InP at room temperature is displayed in dependence of the doping level. The samples were doped with Sn and Zn, respectively. Ellipsometry was used for energies above E_0, whereas the absorption edge itself was investigated by photoluminescence (PL) down to $\alpha \simeq 40$ cm^{-1}. For the PL measurements the samples were excited by 6328 Å radiation of a He-Ne laser. The luminescent light was investigated with a 2-m grating spectrometer and a cooled photomultiplier. The absorption spectrum $\alpha(E)$ was obtained from the PL emission spectrum $I(E)$ via the principle of detailed balance,[32]

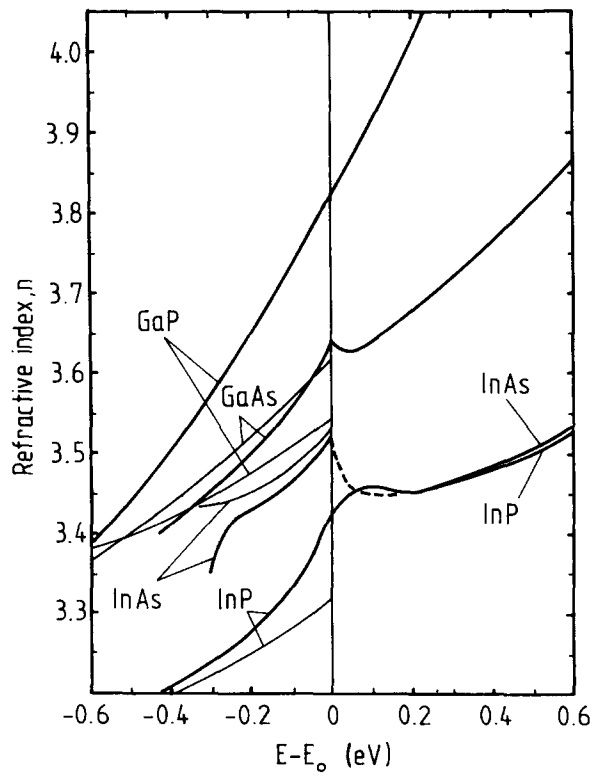

FIG. 4. Magnified section of Fig. 3 around the band gap showing the binary indices of Fig. 3 (thick lines) compared to those calculated after Afromowitz[28] with the single oscillator model parameters taken from Ref. 27 (thin lines).

[This article is copyrighted as indicated in the article. Reuse of AIP content is subject to the terms at: http://scitation.aip.org/termsconditions. Downloaded to] IP: 35.8.11.3 On: Wed, 27 Jan 2016 02:10:42

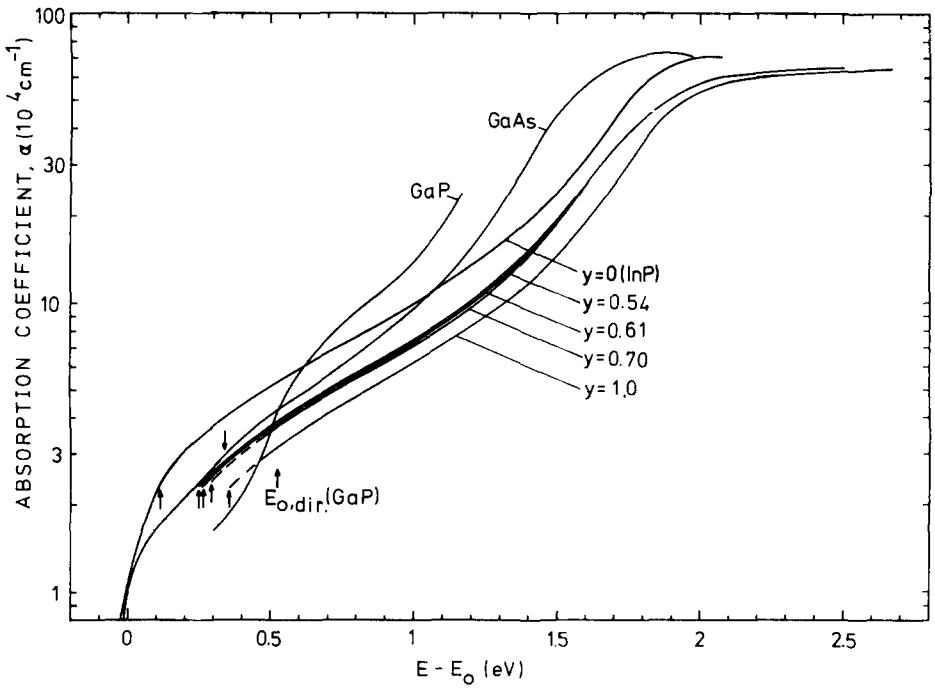

FIG. 5. Measured absorption constants vs $E - E_0$ of GaAs, GaP and $In_{1-x}Ga_xP_{1-y}As_y$. The arrows indicate the respective Δ_0 values.[15] For GaP, $E_0 = 2.26$ eV (indirect gap) was used, and the direct gap is also indicated.

$$\alpha(E) = \frac{h^3c^2[\exp(E/kT) - 1]}{8\pi n^2 E^2} I(E). \tag{4}$$

A marked dependence on the free carrier concentration is observed. With increasing donor concentration the absorption edge is flattened and the gap energy is shifted to higher energies in agreement with the Burstein-Moss effect.

D. Oxide layer thickness

Ellipsometry is a powerful tool to detect thin surface layers such as the natural oxide. The oxide thickness d_{ox} is directly connected with the angle of rotation Δ of the polarization ellipse. This is shown in Figs. 7 and 8 for InP and GaAs. A large variation in d_{ox} between 0.8 and 5.5 nm was found, depending on the surface preparation and the time of exposure to air. In spite of the different oxide thicknesses the

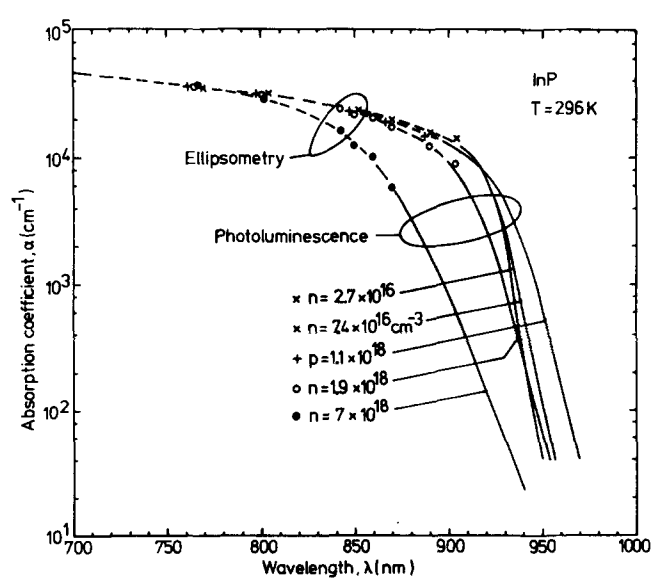

FIG. 6. Absorption constants of differently doped LPE InP samples in the vicinity of the band gap. The dashed curves are drawn through the ellipsometric data points, whereas the full curves are obtained from photoluminescence measurements.

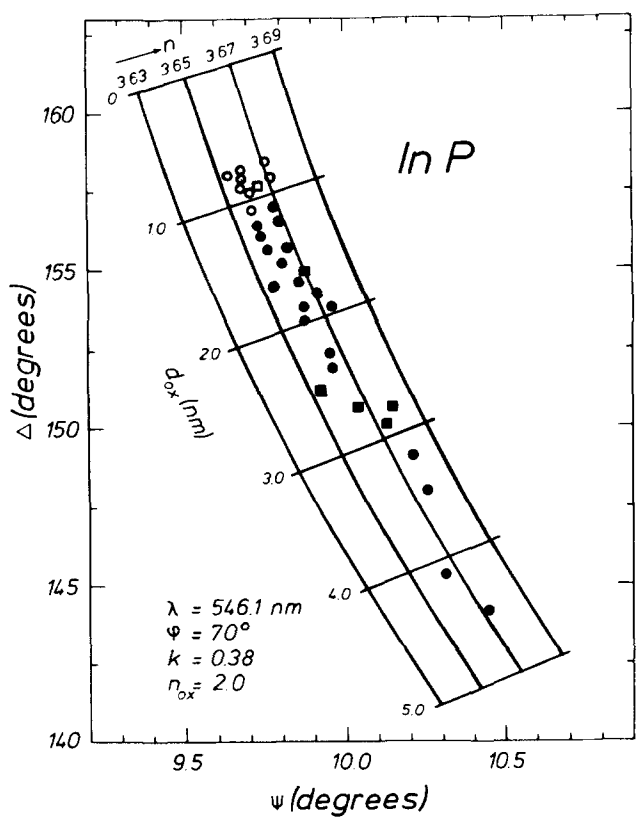

FIG. 7. Refractive index n of various InP samples. It is demonstrated that n is determined to be 3.665 ± 0.010 independent of the thickness d_{ox} of the natural oxide layer. Δ and Ψ are the ellipsometric angles. (□) freshly grown LPE material; (■) air-exposed LPE; (○) freshly etched liquid encapsulated Czochralski (LEC) material; (●) air-exposed LEC. The exposure time of the exposed samples was longer than 1 h in normal laboratory atmosphere.

[This article is copyrighted as indicated in the article. Reuse of AIP content is subject to the terms at: http://scitation.aip.org/termsconditions. Downloaded to] IP: 35.8.11.3 On: Wed, 27 Jan 2016 02:10:42

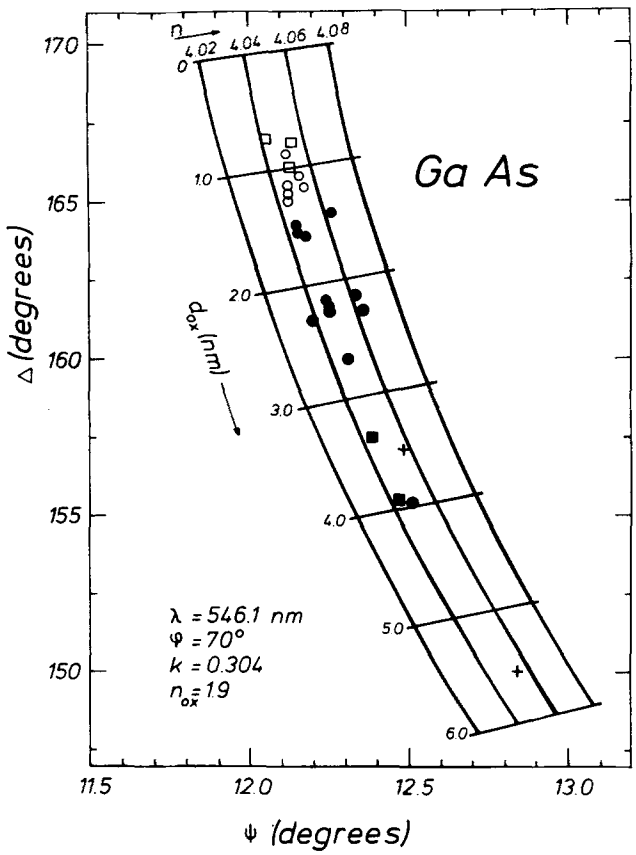

FIG. 8. Refractive index n of various GaAs samples. It is demonstrated that n is determined to be 4.05 ± 0.01 independent of d_{ox} up to 5.5 nm. (□) freshly grown LPE material; (■) air-exposed LPE; (○) freshly etched LEC material; (●) air-exposed LEC; (+) etched and water treated LEC.

refractive index at $\lambda = 546$ nm is determined independently of d_{ox} at a large number of samples to be $n(\text{InP}) = 3.665 \pm 0.010$ and $n(\text{GaAs}) = 4.05 \pm 0.01$, which demonstrates the consistency of the analysis. No difference in n could be found between epitaxial and substrate material.

The angle Δ can also be used to characterize the quality of a substrate cleaning procedure. For InP substrates the following cleaning procedure yielded the largest Δ-values, i.e., the thinnest oxide layers: Degreasing in acetone, deoxidation in HF, etching in 1% Br in methanol, rinsing in methanol and in boiling chloroform. Δ values were as large as those of freshly grown LPE InP layers ($\Delta = 158°$). GaAs substrates were degreased, then etched in H_2SO_4:H_2O_2:H_2O (3:1:1, 50 °C) and finally rinsed in water, propanol, and boiling chloroform. Here again, the cleaning treatment yielded Δ values as large as those of freshly grown LPE GaAs layers ($\Delta = 167°$). A deoxidation step with boiling HCl inserted between the water and the propanol step gave no measurable improvement of the Δ values. A longer treatment in water (30 min), however, is shown to strongly enhance the oxide thickness. Adams and Pruniaux[33] found Δ values up to 166° at the same λ and φ_0 using a different cleaning procedure for their GaAs samples. Thus, these values seem to be the optimum which can be reached by conventional wet cleaning.

The increase of the oxide thickness on two clean InP samples as a function of time exposed to normal laboratory

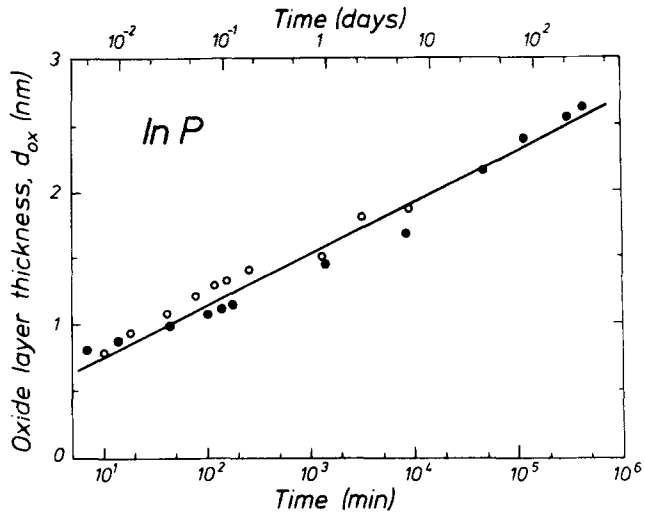

FIG. 9. Thickness of the natural oxide layer on two InP samples ((○) and (●)) as a function of the time exposed to air. The straight line is a fit according to Eq. (5).

air is given in Fig. 9. No saturation of d_{ox} was observed within one year. The thickness can be described by the empirical expression

$$d_{ox} = d_0 \log [(t + t_0)/t_0]. \quad (5)$$

The slope is $d_0 = 0.39$ nm and the parameter $t_0 = (0.12 \pm 0.08)$ min. The accuracy of d_0 depends on the accuracy of $k = 0.38$ taken for InP, as outlined in Sec. II.B. This d_0 is very close to the value 0.41 nm reported for GaAs.[34] Although InP degrades much faster than GaAs at elevated temperatures, it is evident from these data that at room temperature, the surface stability of both compounds is very similar, thus indicating that the quite stable native oxide on InP is In_2O_3 rather than P_2O_5.

IV. CONCLUSION

The optical constants n and k of the system InGaPAs and of the related binary compounds have been determined. The similarity of the dispersion curves of different materials as functions of ΔE together with theoretical considerations on the quantity to be averaged provided the justification for the procedure used to calculate $n_Q(\Delta E, y)$. As $n_Q(\Delta E, y)$ and $\bar{n}_Q(\Delta E, y)$ are given in an analytical form, it is now easy to predict the far-field pattern and the axial-mode separation of quaternary lasers of any wavelength. From the axial-mode separations measured on our own lasers ($\lambda = 1.31\ \mu$m), we got good agreement with Eq. (3) after having included the effect of finite active layer thickness and the InP cladding.

The dependence of the absorption coefficient on carrier concentration given for InP in the vicinity of E_0 (Fig. 6) can be transferred with little error also to InGaPAs. This information together with the measured absorption coefficients of pure samples over the entire composition range of the system InP/InGaPAs (Fig. 5) is useful for the design of photodetectors for the optical communciation.

Finally, some properties of the natural oxide on the layers, namely its thickness and its growth velocity, have been

[This article is copyrighted as indicated in the article. Reuse of AIP content is subject to the terms at: http://scitation.aip.org/termsconditions. Downloaded to] IP: 35.8.11.3 On: Wed, 27 Jan 2016 02:10:42

studied. The quality of a cleaning procedure can easily be judged by the ellipsometric Δ value.

ACKNOWLEDGMENTS

The most valuable technical assistance of K. Orth and H. Westenberger in growing the crystals and of G. Joel in etching the samples is gratefully acknowledged.

[1]G. D. Henshall, P. D. Greene, G. H. B. Thompson, and P. R. Selway, Electron. Lett. **14**, 796 (1978).
[2]Y. Itaya, S. Katayama, and Y. Suematsu, Electron. Lett. **15**, 123 (1979).
[3]G. H. Olsen, C. J. Nuese, and M. Ettenberg, Appl. Phys. Lett. **34**, 262 (1979).
[4]E. Oomura, T. Murotani, M. Ishii, and W. Susaki, Jpn. J. Appl. Phys. **18**, 855 (1979).
[5]P. Chandra, L. A. Coldren, and K. E. Strege, Electron. Lett. **17**, 7 (1981).
[6]M. Cardona, J. Appl. Phys. **36**, 2181 (1965); **32**, 958 (1961).
[7]G. D. Pettit, and W. J. Turner, J. Appl. Phys. **36**, 2081 (1965).
[8]H. R. Philip and H. Ehrenreich, in *Semiconductors and Semimetals*, edited by R. K. Willardson and A. C. Beer, Vol. 3 (Academic, New York, 1967), p. 513.
[9]D. T. F. Marple. J. Appl. Phys. **35**, 1241 (1964).
[10]D. D. Sell, H. C. Casey Jr., and K. W. Wecht, J. Appl. Phys. **45**, 2650 (1974).
[11]A. E. Morgan, Surf. Sci. **43**, 150 (1974).
[12]D. E. Aspnes, *Optical Properties of Solids—New Developments*, edited by B. O. Seraphin (North-Holland, Amsterdam, 1976), p. 799.
[13]E. H. Perea, E. E. Mendez, and C. G. Fonstad, Appl. Phys. Lett. **36**, 978 (1980).
[14]M. Cardona, K. L. Shaklee, and F. H. Pollak, Phys. Rev. **154**, 696 (1967).
[15]P. M. Laufer, F. H. Pollak, R. E. Nahory, and M. A. Pollack, Solid State Commun. **36**, 419 (1980).
[16]E. Kuphal, J. Cryst. Growth **54**, 117 (1981).
[17]J. J. Hsieh, J. Electron. Mater. **7**, 31 (1978).
[18]R. M. A. Azzam and N. M. Bashara, *Ellipsometry and Polarized Light* (North-Holland, Amsterdam, 1977).
[19]H. W. Dinges, Thin Solid Films **50**, L17 (1978).
[20]F. Lukés, Optik **31**, 83 (1970).
[21]H. K. Müller, Phys. Status Solidi **27**, 723 (1968).
[22]E. Kuphal and H. W. Dinges, Res. Inst. German Post Office, Technical Report 14 TBr 9 (1978).
[23]M. Cardona, in *Semiconductors and Semimetals*, edited by R. K. Willardson and A. C. Beer (Academic, New York, 1967), Vol. 3, p. 125.
[24]B. O. Seraphin and H. E. Bennett, in *Semiconductors and Semimetals*, edited by R. K. Willardson and A. C. Beer (Academic, New York, 1967), Vol. 3, p. 499.
[25]R. E. Nahory, M. A. Pollack, Electron. Lett. **14**, 727 (1978).
[26]G. H. Olsen, T. Z. Zamerowski, R. T. Smith, and E. P. Bertin, J. Electron. Mater. **9**, 977 (1980).
[27]J. Buus, M. J. Adams, Solid-State and Electron Devices **3**, 189 (1979).
[28]M. A. Afromowitz, Solid-State Commun. **15**, 59 (1974).
[29]J. W. Harrison and J. R. Hauser, J. Appl. Phys. **47**, 292 (1976).
[30]A. Sasaki, M. Nishiuma, and Y. Takeda, Jpn. J. Appl. Phys. **19**, 1695 (1980).
[31]H. C. Casey, Jr., D. D. Sell, and K. W. Wecht, J. Appl. Phys. **46**, 250 (1975).
[32]W. van Roosbroeck and W. Shockley, Phys. Rev. **94**, 1558 (1954).
[33]A C. Adams and B. R. Pruniaux, J. Electrochem. Soc. **120**, 408 (1973).
[34]E. Kuphal and H. W. Dinges, J. Appl. Phys. **50**, 4196 (1979).
[35]D. E. Aspnes, G. P. Schwartz, G. J. Gualtieri, A. A. Studna, and B. Schwartz, J. Electrochem. Soc. **128**, 590 (1981).

[This article is copyrighted as indicated in the article. Reuse of AIP content is subject to the terms at: http://scitation.aip.org/termsconditions. Downloaded to] IP: 35.8.11.3 On: Wed, 27 Jan 2016 02:10:42